3D Printed Interdigitated Capacitor Based Tilt Sensor

Oliver Ozioko, Habib Nassar, and Ravinder Dahiya, *Fellow, IEEE*

***Abstract*—This paper presents a tilt sensor comprising of 3D printed capacitive sensors located at the four ends of a '+' shaped channel to provide the orientation of objects by using the capacitive fluid level measurement concept. The interdigitated capacitive sensors were developed by 3D printing and the channel was filled with ecoflex and silicone oil to obtain two variants of tilt sensor. The results show a change in the capacitance of ∼11.5% and ∼9.53% for ecoflex and silicone oil-based sensors respectively. A drift of ∼2.6% is observed for ecoflex and ∼0.16% for silicone oil. Considering the lower viscosity and the lower drift, the silicone oil-based tilt sensors were further investigated and two tilt sensors with varying silicone volumes (1 *ml* and 1.5 *ml*) were fabricated and compared for tilt angles ranging from 0° to 30°. The result from all four interdigitated capacitive sensors in the tilt sensing structure show similar rate of change in capacitance (∼0.67% per degree increase in the tilt angle) with a standard deviation of ∼ ±0.1%. However, the sensor with higher volume of silicone oil (1.5 *ml*) saturated at a tilt angle of ∼20° which is ∼10° smaller than the response of the sensor fabricated with 1 *ml* of silicone oil (saturated at 30°). We also demonstrate the possibility of extending the sensor range by optimizing the volume of fluid and the channel's fluid capacity. With integration of fabricated tilt sensor with a robots' body, white cane or smart objects etc., it will be possible to obtain the information about orientation.**

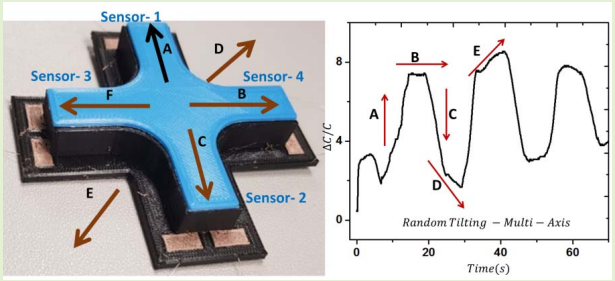

***Index Terms*—3D printing, additive manufacturing, capacitive sensor, tilt sensor, robotics, rehabilitation.**

I. Introduction

THE recent advancement in 3D/4D printing techniques have significantly contributed to the realization of smart and complex systems such as robots [1]–[4], prosthetics [5], [6], DIY ventilators [7], wearable systems as well as human-machine interfaces etc. [8], [9]. 3D printing is an excellent approach for advancing these applications as it allows rapid production of low-cost functional mechanical structures. Further, the advances in the field such as multifunctional 3D/4D printing are opening interesting opportunities for integration of sensors [10], actuators [11] and electronics into complex 3D structures [12]. This is possible as the multimaterial 3D printing allows simultaneous printing of different materials to develop a smart structure [13]–[15] having printed active devices part of their body, instead of conventional placement of off-the-shelf components [3], [15]. This bridges a huge gap in terms of device integration and has the potential to revolutionize several applications, including the ones discussed above. Herein, we use multimaterial 3D printing to develop a fluid-based tilt sensor.

A number of tilt sensors have been reported in literature following various principles (Table I) such as optical [16], [17], fibre Bragg grating [18]–[21], capacitive [22]–[25], thermal, magnetic [26], [27] and electrolytic [28] etc. Amongst them, capacitive sensing [29]–[34] has the advantage of not being affected much by humidity, mechanical misalignment or temperature etc. [23]. Additionally, capacitive sensors require simple readout electronics [29], [35]. Here, we take advantage of the capacitive fluid level sensing technique as well as the flexibility, affordability, and rapid prototyping capability of multimaterial 3D printing to realize capacitive tilt sensors.

The tilt sensor presented here was fabricated with four 3D printed interdigitated capacitive sensors located at the four ends of '+' shaped structure. The four-3D printed capacitive sensors were printed in the channel filled with silicone oil

Manuscript received December 9, 2020; accepted February 7, 2021. Date of publication February 12, 2021; date of current version November 30, 2021. This work was supported in part by the Engineering and Physical Sciences Research Council (EPSRC) Fellowship for Growth under Grant EP/M002527/1 and Grant EP/R029644/1 and in part by the European Commission through Future Emerging Technologies Project PH-CODING under Grant H2020-FETOPEN-2018-829186. This article was presented at the IEEE International Conference on Flexible and Printable Sensors and Systems (FLEPS), 2020. The associate editor coordinating the review of this article and approving it for publication was Prof. Arokia Nathan. *(Corresponding author: Ravinder Dahiya.)*

The authors are with the Bendable Electronics and Sensing Technologies (BEST) Group, James Watt School of Engineering, University of Glasgow, Glasgow G12 8QQ, U.K. (e-mail: ravinder.dahiya@glasgow.ac.uk).

This article has supplementary downloadable material available at https://doi.org/10.1109/JSEN.2021.3058949, provided by the authors.

Digital Object Identifier 10.1109/JSEN.2021.3058949

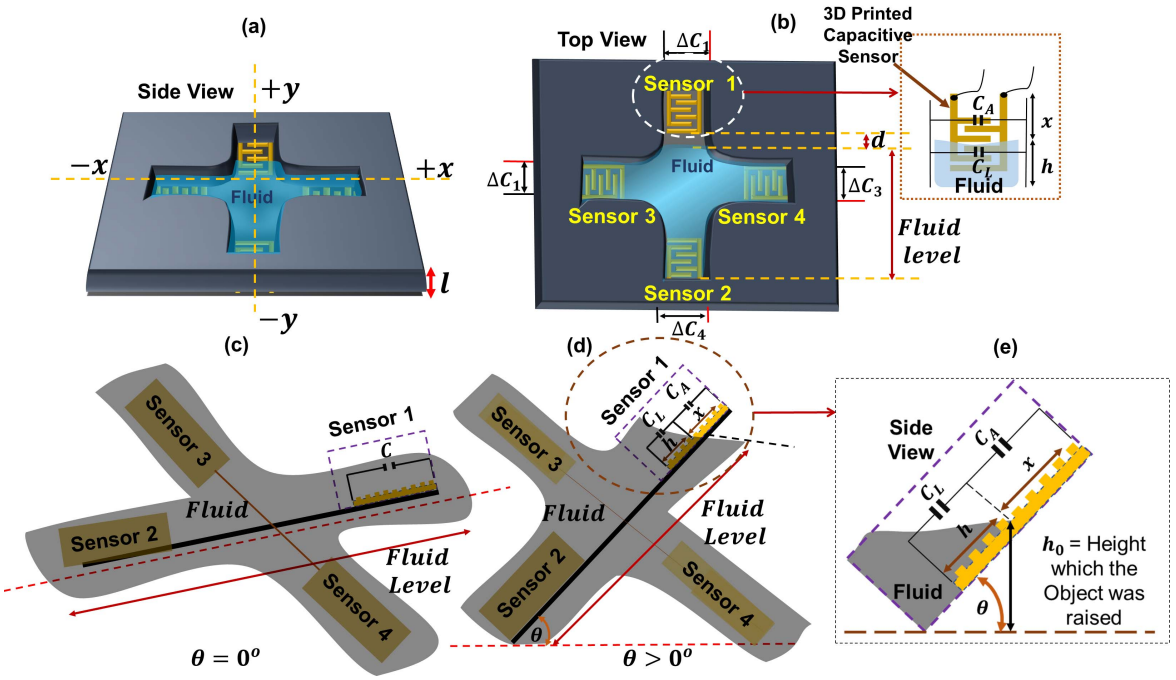

Fig. 1. Device Structure and working principle (a) Side view of tilt sensor (b) Top view of tilt sensor (c) tilt sensor at rest position with angle of inclination $\Theta = 0°$ (d) tilt sensor with angle of inclination $\Theta > 0°$ (e) Details of the structure and operating principle using sensor 1 as reference.

TABLE I
COMPARISON DIFFERENT COMMONLY USED TILT SENSORS

Working Principle	**Material**	**Sensitivity**	**Tilt Range**	**Ref.**
Magnetic	Magnetic Fluid	0.004°	±10	[27]
Fibre Bragg Grating	Optical Fibre	1.1pm/° up to 408.3 pm/◦	±20° up to ±90°	[18-21, 36]
Electrolytic	Graphite in PDMS	0.02V/°	±40°	[28]
Capacitive	Movable electrodes	13 fF/°	±50°	[25]
Capacitive	**Silicone Oil**	**0.67%/°**	**±30°**	**This Work**

(Fig. 1). The capacitive sensors are located at the –x, +x, -y and +y axes, as shown in Fig. 1, to measure the orientation in both the x and y axes using the concept of capacitive fluid level measurement. To achieve this, we first fabricated four similar interdigitated capacitive sensors using multimaterial 3D printing and carried out a comparison of their fluid level sensing capability using Ecoflex and silicone oil.

We characterized each of the four sensors separately to understand their performance and the variation of capacitance when the fluid (Ecoflex – only part A, or silicone oil) is in contact with the electrodes. With this, we made appropriate design choices with regards to printing settings, appropriate fluid type, and volume of fluid necessary to realize the proposed tilt sensor. The findings were then utilized to fabricate the 3D printed tilt sensor using silicone oil as the tilting fluid, Silicone oil is six times less viscous (500cps), and hence shows lower drift in comparison with Ecoflex™ (3000cps). This is an extension of our previous work [37]. Previously we utilized only Ecoflex as a tilting fluid and only tested for a tilt range of -20° to +20°. In this work, we carried out more analysis of the Ecoflex-based sensor and compared its performance with a newly fabricated tilt sensor realize with a silicone oil (a less viscous fluid). We equally extended the tilt range up +30° and investigated a possibility to extend this range even further by varying fluid volume and the channel's fluid capacity. The fabricated tilt sensor could be used as part of a robotic hand or smart objects for the detection of their orientation as may be required.

This paper is organized as follows: The device structure and working principle are described in Section II. The fabrication of the device is presented in Section III, followed by the characterization studies in Section IV. Results and discussions are presented in Section V, and key outcomes of the paper are finally summarized in Section VI.

II. DEVICE STRUCTURE AND OPERATING PRINCIPLE

Fig. 1 shows the structure of the fabricated tilt sensor and its working principle. It comprises of four similar 3D printed capacitive sensors embedded in a silicone fluid-filled channel of depth l (Fig. 1a and 1b). The housing of the channel and the capacitive sensors are all printed as one structure using multimaterial 3D printing techniques [38], [39]. The sensor utilizes the principle of capacitive fluid level sensing to determine the orientation of any object it is attached to. Two opposite sensors are utilized to measure the orientation in one axis (sensors 1 and 2 measures orientation in the $+y$ and $-y$ axes, sensors 3 and 4 measures the orientation in $-x$ and $+x$ axes respectively). At rest state, we assume the tilt angle *O to be 0°* (Fig. 1c) and the height which the object is raised to h_o *to be 0.* In this case, the fluid inside the channel will be at a rest state and completely covering all the sensors (sensor 1 to

4, Fig. 1c). Under this condition, the change in capacitance for all the sensors ΔC_1, ΔC_2, ΔC_3, ΔC_4, is recorded as outputs for sensors 1, 2, 3 and 4 respectively. This is noted and recorded as the initial value. When the sensor is tilted ($O > 0°$, Fig. 1d) towards sensor 2, for instance, the fluid flows away from sensor 1 (Fig. 1d) towards sensor 2. As the fluid flows away from sensor 1, the level of fluid (h) covering the sensor (Fig.1d) reduces and the capacitance changes proportionally. Therefore, this level of fluid (h), and the height by which the object is raised (h_o) are used to estimate O, the current orientation of the device (Fig. 1e), using equation 1. Similarly, the object orientation for other axis is estimated using sensors 3 and 4. So, by simultaneously observing the output values of sensors 1, 2, 3 and 4, we can determine the object orientation using equation (1). This is similar to the equation used for capacitive fluid level measurement techniques in which the capacitance is directly related to the level of fluid in contact with the sensor (Equation (1), Fig. 1e).

$$Sin O = ho/h(1) \tag{1}$$

where, h_o is the height that the object is raised above the rest position, and h (the level of fluid covering the sensor) is calculated from Equation 2 using the value of the capacitance measured in each case.

$$C = C_A + C_L \tag{2}$$

where C is the measured capacitance of each of the sensors (ΔC_1, ΔC_2, ΔC_3, ΔC_4), C_A is the capacitance of the area of the sensor without fluid (x), and C_L is the capacitance of the area of the sensor with fluid (h). Other important considerations are the depth of the fluid channel l (Fig. 1a), the volume of fluid in the channel and the distance d (Fig. 1b). The distance d (Fig. 1b) is dependent on the volume of the fluid in the channel and determines the distance the fluid has to flow to touch the electrodes for capacitance to change. However, d is taken care of by choosing the right volume. So the volume and/or the depth of the channel determines how much space the fluid has to flow and could impact the range of the tilt angle that the sensor is able to provide as we investigated and presented in this work.

III. Fabrication

The multi-nozzle Ultimaker S5 (Ultimaker B.V., Netherlands) FDM 3D printer is used for the fabrication of both the four similar interdigitated capacitive sensors as well as the tilt sensor presented here. The first nozzle of the 3D printer is loaded with standard polylactic acid (PLA) which serves as the build material for the sensor structure (Fig. 2a and 2b). The second nozzle is loaded with a commercial conductive polymer composite (Electrifi, Multi3D, USA). The Electrifi filament is made of a biodegradable polyester and copper composite which has a melting temperature of 60°C. The conductive filament is used to print the interdigitated electrodes that offer the capacitive tilt-sensing functionality, as well as the pads for external wiring (Fig. 2c and 2g).

The conductive composite is printed in 'grooves' designed in the PLA structure (Fig. 2b and 2f). As the print progresses layer-by-layer upwards, PLA and Electrifi are deposited from the nozzles to create the desired shape. The contact pads are printed on a different layer to the electrodes and the housing of the fluid. Each pair of electrodes are connected to their contact pads via vertical, out-of-plane interconnections printed within the PLA housing (Fig. 2e). The vertical connections have a cross-sectional area of $1mm^2$.

The PLA is printed at 200°C at a speed of $50mms^{-1}$. The Electrifi is printed at 150°C at a speed of $5mms^{-1}$. All the Electrifi layers are printed as bottom layers specified in the slicer software Cura. Doing so, provides a better connection between the deposited rasters from the nozzle ensuring stronger adhesion and a higher and more consistent conductivity. Both nozzles used are 0.25mm in diameter and the materials are printed at a 0.1mm layer height. The small nozzle diameters ensure that the smaller features of the print are preserved and are not causing electrical shorting. These are the 1mm wide electrodes, the 1mm spacing between them, and the vertical interconnects (Fig. 2f and 2g). A prime tower is used to ensure both materials are consistently flowing through the nozzles at the side of the build plate before depositing more material on the print structure. To ensure the structure adheres well to the build plate and maintains its integrity, the print bed is kept at 40°C throughout and blue painter's tape is placed on the bed.

Thin wires are used as external electrical connections for characterizing the sensor. They are attached to the tilt sensor contact pads. To make the connection, the print is paused during the printing of the pads. A wire is placed on the contact pad and silver paste (RS Pro 186-3600, RS Components, UK) is applied between the wire and the printed conductive material (Fig. 2d). The silver paste works to reduce the contact resistance between the wire and the Electrifi. The silver paste is left to dry while the structure is still on the print bed for around 30mins. The print is then resumed allowing the subsequent layers of conductive material to print on top of the wire and dried ink (Fig. 2e). This technique decreases the contact resistance between the printed Electrifi and external connectors and allows the wires on the contact pads to be securely attached to the printed structure during handing and tilting. After printing, the channel was filled with fluid using a syringe and a plus-shaped 3D printed cover tightly bonded on top to cover the fluid.

Two versions of tilt sensors were fabricated with the main difference being the volume ($1.5ml$ and $1ml$) of silicone oil in the channel varied. This was done to evaluate the effect of varying the volume of fluid in the channel. Intuitively, we anticipate that the volume of fluid in the channel will affect the range of the sensor as the fluid will have less space to flow during tilting and this could saturate the output of the sensor quickly. For instance, if the channel is fully filled with fluid, the active regions of all the sensors in the channel will be completely immersed in the fluid. This means that when the sensor is tilted, there will be no change in the level of fluid and hence capacitance. Similarly, by filling the channel with a small volume of fluid could leave the sensors showing a very low change in the capacitance. The characterization of the two versions of the tilt sensor (with $1ml$ and $1.5ml$ fluid

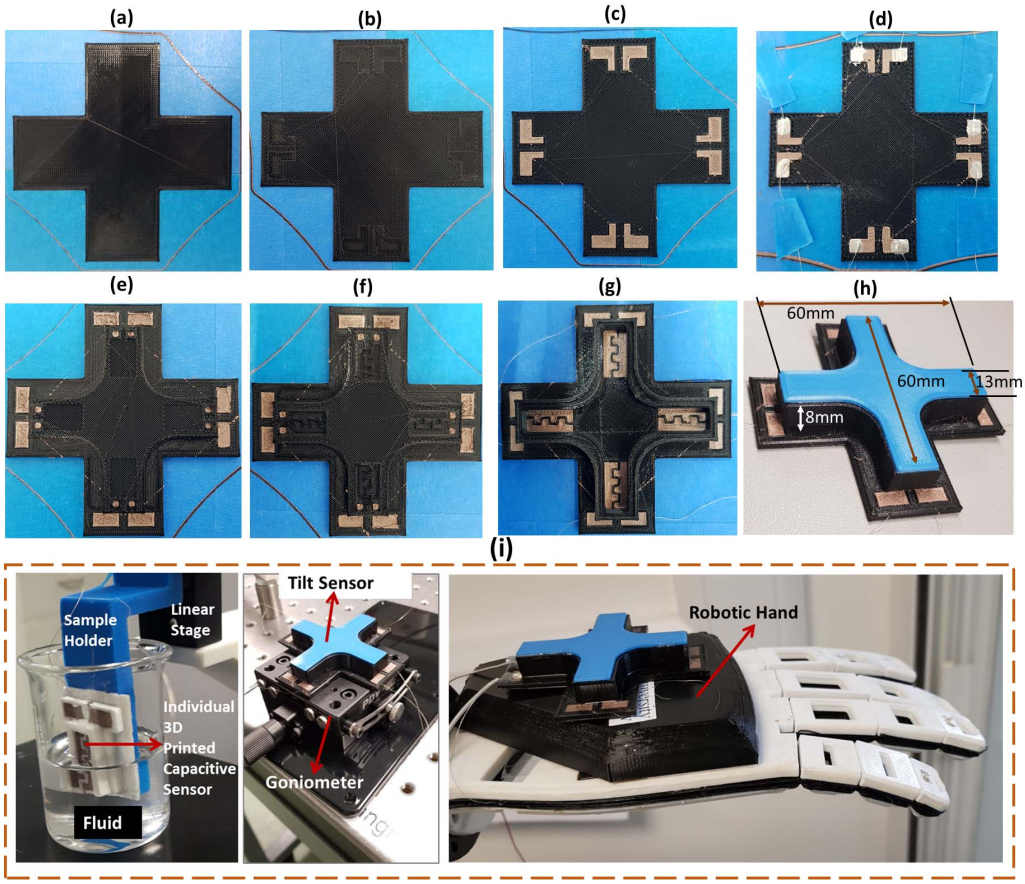

Fig. 2. The fabrication stages of the 3D printed tilt sensor (a) The base PLA layer (b) The base layer with grooves in the structure for the contact pads (c) The printed conductive contact pads using the Electrifi filament (d) The placement of external wires and silver ink on the contact pads (e) The printing of the vertical interconnections to the fluid-filled channel (f) The channel with grooves in the PLA for the interdigitated electrodes (g) The completed printed interdigitated capacitive electrodes in the channel (h) A side view of the tilt sensor with a PLA cover for the channel (i) Setup for the tilt sensor characterization.

volume) is presented later in this work and provides some justification for this.

IV. Characterization

The characterization carried out in this work could be classified into two parts: (1) Characterization of the four similarly fabricated interdigitated capacitive sensors using Ecoflex™ and silicone oil (Dimethicone). This involved several dip and remove cycles of each of the sensors in Ecoflex™ as well as silicone oil and then a comparison of both to see their reproducibility. This leads to the choice of appropriate parameters for the tilt sensor fabrication; (2) Characterization of the fabricated tilt Sensor. This involves the tilting of the two fabricated tilt sensors (with $1ml$ and $1.5ml$ of fluid) to different angles -30^o to +30^o, random tilting of the sensor, and an experiment for extension of the tilting range.

A. Characterization of Individual Capacitive Sensors

The four fabricated individual capacitive sensors were characterized using a dip and remove cycle to understand the performance of the 3D printed sensor in fluids of different viscosities: (Ecoflex Part-A, 3000cps) and silicone oil (Dimethicone, 500cps). In each case, the sensors were firmly attached to a computer-controlled linear stage which has a linear motor with ∼0.1mm displacement resolution. The sensors were then connected to an E4980AL precision LCR meter (Keysight Technologies, Santa Clara, CA, USA) which is connected to a computer running a custom-made LabVIEW 2018 Robotics v18.0f2 program (National Instruments, Texas, USA) to measure the capacitance of each sensor and control the linear stage. First, the sensors were each dipped into ∼15ml Ecoflex systematically using the LabVIEW program, at a step of 1mm until the sensors' active region (∼12mm) was fully submerged and the output saturated. This was carried out to investigate the change in capacitance for different fluid levels as this is the basis of operation of the proposed fluid-based tilt sensor. It enabled us to understand the repeatability of the four similarly fabricated sensors. Next, one of the interdigitated capacitive sensors was used to compare the performance of Ecoflex™ and silicone oil to choose a suitable fluid for the intended tilting application. This was carried out using the same dip and remove procedure used for the characterization of the four individual sensors. Sensor-1 was used for this purpose and was systematically dipped into ∼$15ml$ of silicone oil ((Dimethicone) at the same 1mm step and then gradually unloaded at the same step. To understand the stability of the sensors and their repeatability, we carried out cyclic loading of

sensor-1 in Ecoflex and silicone oil at ∼0.33Hz, and ∼0.625Hz for over 100 cycles. The chosen frequency allows sufficient time for fluid to away from sensor's active area for better comparison.

B. Characterization of Tilt Sensor

Based on the results of characterizing the individual capacitive sensors, the tilt sensor was fabricated with silicone oil which has about six times less viscosity than Ecoflex and hence less drift. The characterization of the tilt sensor is presented in this section and could be divided into three parts; 1) Tilting the sensor from 0° to 40° on x and y-axes; 2) Random tilting of the sensor to different axes and 3) Characterization of the sensor for a larger tilt range (up to 50°).

1) Tilting of the Sensor From 0° to 40° on x and y-axes: Here, we tilted the two tilt sensors (sensor with 1.5*ml* and that with 1*ml* fluid) using different angles (0° to 40°) in both the x- and y-axes and recorded the output of corresponding sensor. The tilting was done using a goniometer from Owis (Germany) with a 0.1° knob (Fig. 2i). In each case, one of the interdigitated capacitive sensors that make up the tilt sensor was used as a reference point and the change in capacitance as the fluid flows to and away from this reference sensor was recorded using an E4980AL precision LCR meter (Keysight Technologies, Santa Clara, CA, USA). The tilt sensor was firmly attached to the goniometer and the reference sensor connected to the LCR meter. The LCR meter is then connected to a computer running a custom-made LabVIEW 2018 Robotics v18.0f2 program (National Instruments, Texas, USA) to measure the change in capacitance for every tilt angle.

2) Random Tilt to Different Axes: The performance of the tilt sensor was observed for random tilt angles on a single axis (+x and –x axes) as well as to multiple random axes. The tilt sensor was first mounted on a 7 × 5cm 3D printed material and sensor 1 connected to the LCR meter to read its output. The LCR meter is then connected to a computer running a custom-made LabVIEW 2018 Robotics v18.0f2 program (National Instruments, Texas, USA) to measure the change in capacitance for every tilt angle. By attaching the tilt sensor to a custom-made robotic hand, (*Supporting video S1),* the sensor was tilted for the fluid to flow to the reference sensor and away from the reference sensor in different orientations while the output was automatically logged on the computer. A similar procedure was used to tilt the sensor randomly at different orientations to see how it can respond to randomly varying orientation *(Supporting video, S2*).

3) Characterization of Sensor for Larger Tilt Range (Up To 50°): We carried out further characterization using one single fabricated interdigitated capacitor to verify that the depth of the channel could affect the space the fluid has to flow in the 3D printed channel and hence influence the measurable tilt angle range. We utilized a larger volume of fluid (∼15ml) in a channel with bigger fluid capacity (∼30ml). One of the 3D printed interdigitated capacitive sensors was utilized to demonstrate that the tilt range can be increased by increasing the channel's fluid capacity, above what we used here (>3*ml*). This was carried out by firmly attaching the interdigitated capacitive sensor (fabricated as described in Section 3) vertically inside a 3D printed material (with ∼30*ml* fluid capacity). Silicone oil was poured inside to just cover ∼25% of the sensor's active region. The sensor was then connected to an LCR meter as described in Section IV (B) above. The 3D printed material was then tilted at angles 5° up to 50° in steps of 5° and its output recorded also as described in Section IV (B).

V. Results and Discussion

A. Individual 3D Printed Capacitor

Fig. 3 shows the result of characterization of the individual capacitive sensors using Ecoflex™ and silicone oil (Dimethicone). Fig. 3a shows the result of the dip and release characterization of the four similarly fabricated interdigitated 3D printed capacitors. It shows a relative change in capacitance of ΔC/C ∼0.67% per mm. A comparison of the four sensors shows a standard deviation of ∼0.33% part of which is due to some degree of non-uniformity in the 3D printed structures. However, the effect is not significant given that the sensors are individually measured during tilt operation. Fig.3b shows loading and unloading of the sensors carried out to compare the performance of Ecoflex and silicone oil (Dimethicone). It is observed that Ecoflex™ has a higher change in capacitance (ΔC/C ∼11.5%) in comparison to that of silicone oil (ΔC/C ∼9.53%). Considering points A and B (Fig. 3b), a drift of ∼2.6% is observed for Ecoflex and ∼0.16% for silicone oil. This drift is primarily due to the higher viscosity of the (Ecoflex™, ∼3000cps) which is about six times that of the silicone oil (∼500cps). Considering the intended tilting application, the lower the viscosity, the faster the fluid can flow to and out of the sensor's active region and hence increasing its response and recovery time. This makes silicone oil the better choice in this case.

Fig. 3c and Fig. 3d show the cyclic response of the sensor using both Ecoflex™ and silicone oil. During the cyclic loading of the sensor at 0.33Hz, it could be seen from points *P* and *Q* of Fig. 3c that the sensor assumes a new base line once the cycles starts. This is due to the fact that some all the fluid do not leave the sensor's active area completley. This new base line is also seen to be higher for Ecoflex™ (∼4.5% drift) in comparison to silicone oil (∼2.1% drift) due to the higher viscosity of Ecoflex™ as mentioned earlier. However, in both cases the sensor is able to always return to the new base line until the end of the cycle when all the fluid is allowed to recover by allowing the fluid to leave the surface of the sensor. Examining ths recovery time shows ∼5.35s for Ecoflex™ and ∼2.18s for silicone oil. Following this, we utilized silicone oil in the realization of the tilt sensor presented in this work.

B. Tilting Sensor From 0° to 40° on x and y-Axes

Fig. 4a shows the image of the fabricated tilt sensor and Fig. 4b shows the result of the two fabricated tilt sensors (sensor with 1.5*ml* and 1*ml* of silicone oil) at angles ranging from 0° to 40° for both x – and y –axes. The sensor structure shown in Fig. 4a indicates that for a full range on each axis, the sensors in the opposite directions are used. For instance, sensor-1 measures the orientation for 0° to +40 while sensor-2 measures the orientation for 0° to -40°. Similarly, sensor-3 measures for 0 to -40 while sensor-4 measures orientation

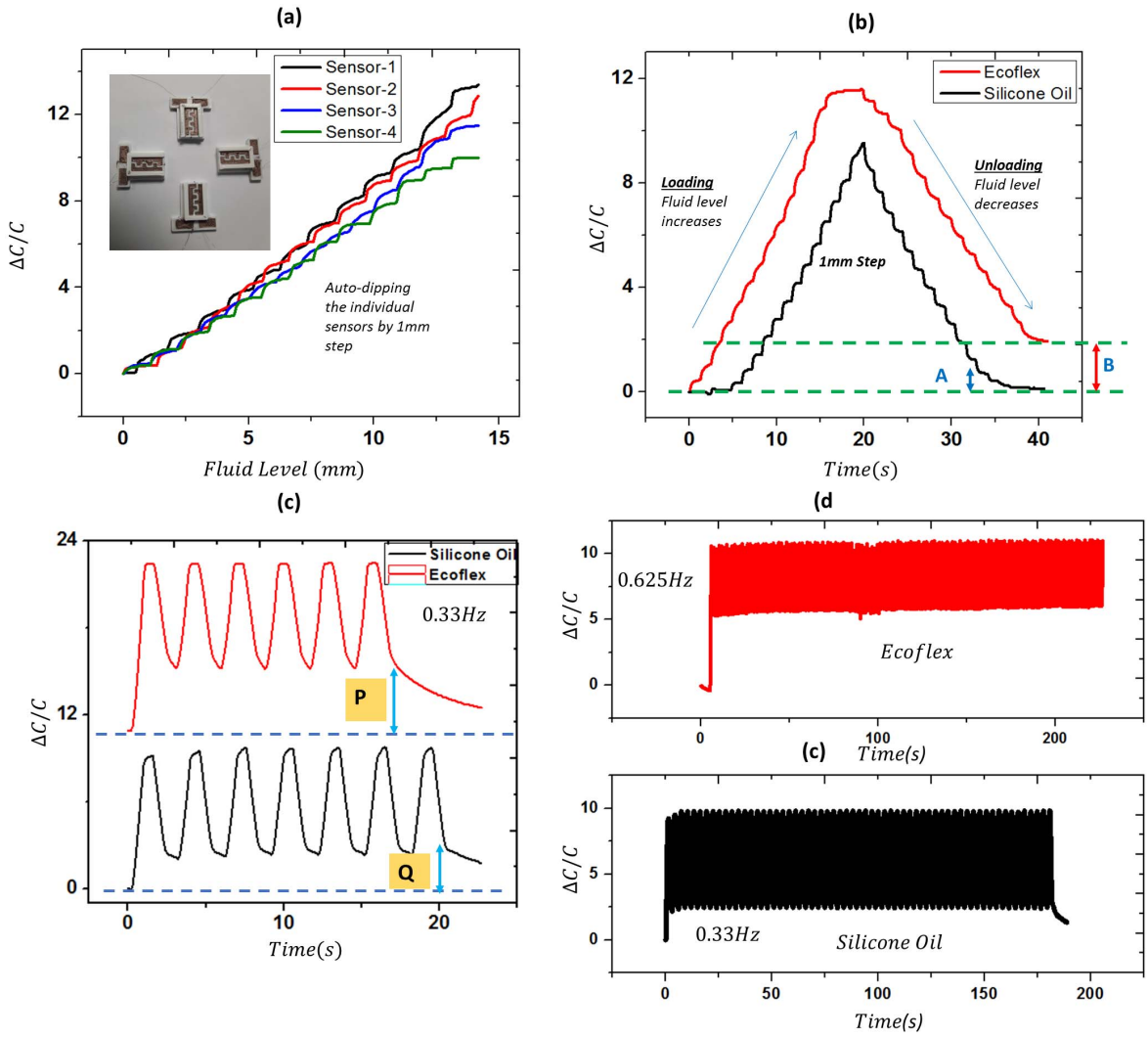

Fig. 3. (a) Change in capacitance for different fluid levels (b)+ loading and unloading of individual sensor using Ecoflex™ and silicone oil (c) Cyclic response of the sensor using Ecoflex™ and silicone oil at 0.33Hz (d) Cyclic loading at 0.33Hz and 0.625Hz.

for 0^o to $+40^o$. The results in Fig. 4b show the same rate of change in capacitance ($\sim$0.67% per degree increase in tilt angle) with a standard deviation of $\sim \pm 0.1\%$ for all the four sensors. However, the sensor with higher volume of silicone oil ($1.5ml$) saturated at a tilt angle of $\sim 20^o$ which is $\sim 10^o$ smaller that of the sensor fabricated with $1ml$ of silicone oil (saturated at 30^o). This is attributed to the fluid not having much room to flow inside the channel. Fig. 4c shows the result of tilting the sensor-1 and 2 to observe the reproducibility across one full axis (-x to +x) and this shows that both sensors have a similar response and can measure orientation on this axis during continuous tilting.

C. Random Tilting

Fig. 4d shows the different orientations that the sensor was tilted to, with one of the sensors taken as a reference point. These orientations are represented as A to E for easy reference. Fig. 4e is a case where the sensor is tilted to and from the +y and –y axis. In this case, the fluid flows away from the reference sensor which leads to decrease in capacitance of the sensor, when it is tilted back; the capacitance gradually increases (Fig. 4e). In addition to tilting the sensor only in the positive and negative y-axis, the sensor was also randomly and continuously tilted to different orientations. Fig. 4f shows the result of tilting the sensor for the different orientations (shown in Fig. 4d) with one of the sensors taken as a reference point. This summarizes the response of the sensor under continuous tilt to different orientations back and forth. Point A shows that when tilted to the negative y-axis (Fig. 4d2) the fluid flows towards the reference sensor and the capacitance will begin to increase. However, when the sensor is tilted to the positive x-axis (Fig. 4d3) the capacitance remains nearly constant as the level of fluid on the reference sensor is not changing significantly *(Supporting video, S2)*. Point C is a case when the sensor is tilted towards the positive y-axis (Fig. 4d4), this causes the fluid to flow away from the reference sensor and hence a decrease in the capacitance is recorded. Point D shows the orientation of the sensor as shown in Fig. 4d5 (towards +y-axis and +x-axis) causing the fluid to flow away from the sensor and a decrease in capacitance observed. This is

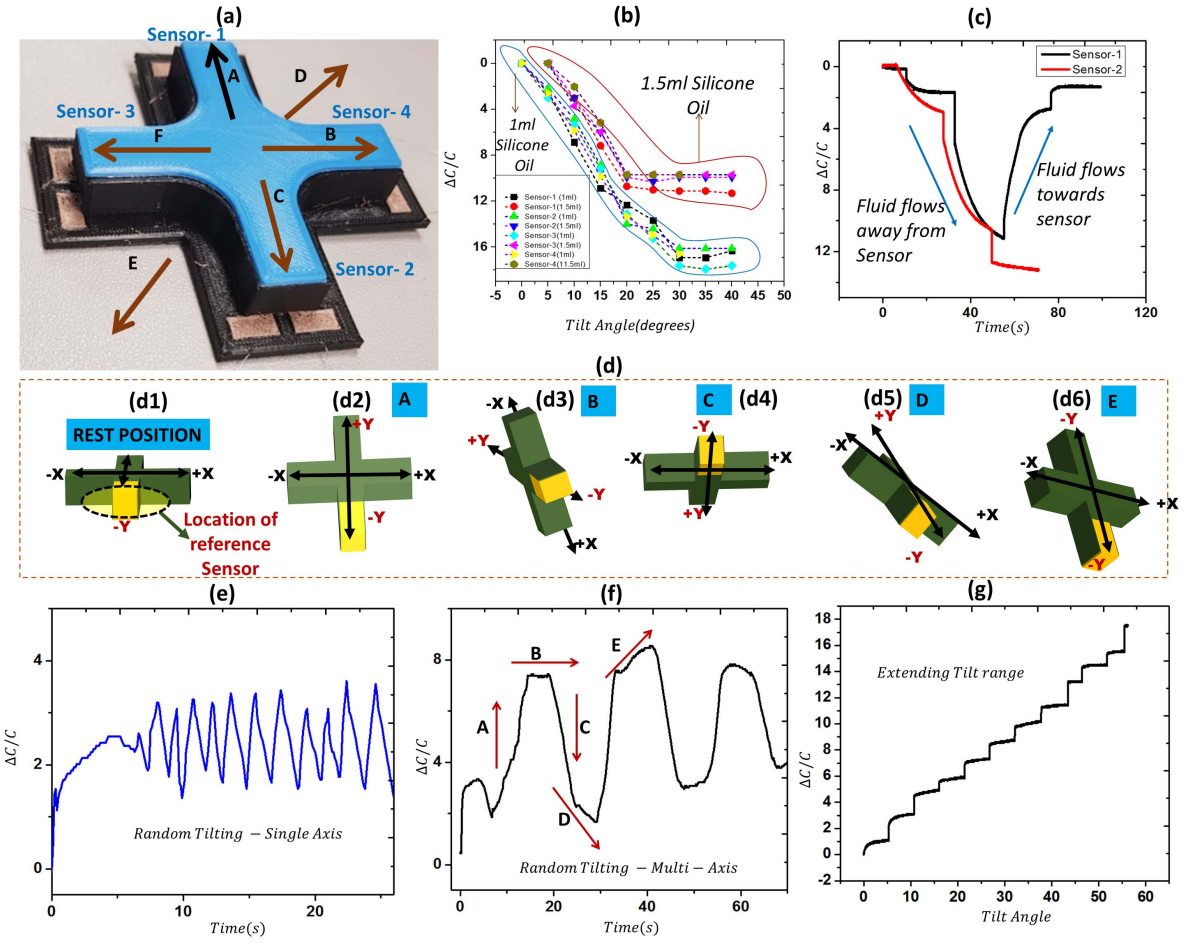

Fig. 4. (a) Fabricated tilt sensor, (b) Response of the two tilt sensors fabricated with 1.5ml and 1ml silicone oil, showing the change in capacitance per degree rise in tilt angle, (c) Reproducibility of sensor 1 and 2 when tilted to the –x and +x-axis, (d) Different orientations for characterization of the tilt sensor, (e) Random tilt of the sensor to the +x and –x axis, (f) Response of the tilt sensor under continuous tilt to different orientations as depicted in Fig. 4d, (g) Result of characterizing the interdigitated capacitive sensor for larger tilting range.

like point E but in opposite direction as shown in Fig. 4d6 (between +x and –y-axis). In the case of both points D and E the fluid flows away much more in a gradual way because the sensor is tilted between two different axes. Point F shows the case when the fluid is tilted to the –x axis causing the fluid level on the reference sensor to be relatively constant and hence a constant change in capacitance was observed. As expected, the capacitance of the reference sensor was relatively constant when tilting to –x- axis and +x-axis, this is required because orientation to this axis will be measured by observing the change in the output of sensors 3 and 4 respectively. Fig. 4g shows the result of characterizing the fabricated sensors for an extended range up to $\sim 50^{o}$or more. We carried this out to show that by increasing the size of the channel's fluid capacity above what we utilized (>3ml), the sensor's range could be further extended. This is because there is more room for the fluid to flow when tilted and hence, the saturation of the output is delayed.

VI. Conclusion

In this work, we have presented 3D printed interdigitated capacitive sensors usable for fluid level measurement and a fluid-based tilt sensing application. First, we fabricated and investigated the performance of four similar 3D printed interdigitated capacitors to understand their characteristics. Using the results, we fabricated and compared two fluid-based 3D printed tilt sensors and characterized them using Ecoflex^{TM} and silicone oil as the tilting fluid. The results show more drift for Ecoflex ($\sim$4.1%) in comparison to silicone oil (2.1%). Utilizing silicone oil as the tilting fluid showed the ability to sense a tilt angle of $\sim \pm 30^{0}$, or more depending on the volume of fluid and size of the 3D printed channel. We figured that the range of the sensor could be extended by either increasing the volume of the channel in which the fluid moves during tilt or reducing the volume of fluid in the channel. The study carried out in this work finds application in robotics as well as in fluid level sensing in which the sensor and the fluid container could be 3D printed as one structure. Effect of temperature on the sensor performance would be studied as part of future work and the performance of the sensor could be further improved by utilizing other types of fluids with lower viscosities. To demonstrate its practical use, future work will also involve the utilization of the results to 3D print the tilt sensor as part of a robotic hand and interpret the output of the sensors using artificial intelligence.

REFERENCES

[1] H. Ota *et al.*, "Application of 3D printing for smart objects with embedded electronic sensors and systems," *Adv. Mater. Technol.*, vol. 1, no. 1, Apr. 2016, Art. no. 1600013.

[2] S.-Z. Guo, K. Qiu, F. Meng, S. H. Park, and M. C. McAlpine, "3D printed stretchable tactile sensors," *Adv. Mater.*, vol. 29, no. 27, Jul. 2017, Art. no. 1701218.

[3] M. Ntagios, H. Nassar, A. Pullanchiyodan, W. T. Navaraj, and R. Dahiya, "Robotic hands with intrinsic tactile sensing via 3D printed soft pressure sensors," *Adv. Intell. Syst.*, vol. 2, no. 6, Jun. 2020, Art. no. 1900080.

[4] E. S. Keneth, A. Kamyshny, M. Totaro, L. Beccai, and S. Magdassi, "3D printing materials for soft robotics," *Adv. Mater.*, Nov. 2020, Art. no. 2003387, doi: 10.1002/adma.202003387.

[5] J. Koprnicky, J. Šafka, and M. Ackermann, "Using of 3D printing technology in low cost prosthetics," in *Materials Science Forum*, vol. 919. Freienbach, Switzerland: Trans Tech Publications, 2018, pp. 199–206.

[6] R. Chirila, M. Ntagios, and R. Dahiya, "3D printed wearable exoskeleton human-machine interfacing device," presented at the IEEE Sensors Conf., Rotterdam, The Netherlands, Oct. 2020.

[7] A. Christou, M. Ntagios, A. Hart, and R. Dahiya, "GlasVent—The rapidly deployable emergency ventilator," *Global Challenges*, vol. 4, no. 12, Dec. 2020, Art. no. 2000046.

[8] R. Dahiya, "E-Skin: From humanoids to humans," *Proc. IEEE*, vol. 107, no. 2, pp. 247–252, Feb. 2019.

[9] R. Dahiya *et al.*, "Large-area soft e-skin: The challenges beyond sensor designs," *Proc. IEEE*, vol. 107, no. 10, pp. 2016–2033, Oct. 2019.

[10] M. Soni, M. Bhattacharjee, M. Ntagios, and R. Dahiya, "Printed temperature sensor based on PEDOT: PSS-graphene oxide composite," *IEEE Sensors J.*, vol. 20, no. 14, pp. 7525–7531, Jul. 2020.

[11] O. Ozioko, P. Karipoth, P. Escobedo, M. Ntagios, A. Pullanchiyodan, and R. Dahiya, "SensAct: The soft and squishy tactile sensor with integrated flexible actuator," *Adv. Intell. Syst.*, Jan. 2021, Art. no. 1900145, doi: 10.1002/aisy.201900145.

[12] D. Espalin, D. W. Muse, E. MacDonald, and R. B. Wicker, "3D printing multifunctionality: Structures with electronics," *Int. J. Adv. Manuf. Technol.*, vol. 72, nos. 5–8, pp. 963–978, May 2014.

[13] Z. Zhu, D. W. H. Ng, H. S. Park, and M. C. McAlpine, "3D-printed multifunctional materials enabled by artificial-intelligence-assisted fabrication technologies," *Nature Rev. Mater.*, to be published.

[14] H. Nassar, M. Ntagios, W. T. Navaraj, and R. Dahiya, "Multi-material 3D printed bendable smart sensing structures," in *Proc. IEEE Sensors*, Oct. 2018, pp. 1–4.

[15] A. Bandyopadhyay and B. Heer, "Additive manufacturing of multi-material structures," *Mater. Sc. Eng, R, Rep.*, vol. 129, pp. 1–16, Jul. 2018.

[16] J.-H. Wu, K.-Y. Horng, S.-L. Lin, and R.-S. Chang, "A two-axis tilt sensor based on optics," *Meas. Sci. Technol.*, vol. 17, no. 4, pp. N9–N12, Apr. 2006.

[17] C. Zhu and J. Huang, "Smart fiber-optic inclinometer," in *Proc. Conf. Lasers Electro-Optics*, May 2020, pp. 1–2.

[18] C. Hong, Y. Zhang, and Z. A. Abro, "A fiber Bragg grating-based inclinometer fabricated using 3-D printing method for slope monitoring," *Geotech. Test. J.*, vol. 43, pp. 38–51, 2020.

[19] B. Ruan, Y. Hao, H. Kang, Q. Shen, and H. Chang, "A mode-localized tilt sensor with resolution of 2.4e-5 degrees within the range of 50 degrees," in *Proc. IEEE Int. Symp. Inertial Sensors Syst. (INERTIAL)*, Mar. 2020, pp. 1–4.

[20] K. Li, Y. Zhao, Y. Li, G. Liu, and J. Li, "Fiber Bragg grating biaxial tilt sensor using one optical fiber," *Optik*, vol. 218, Sep. 2020, Art. no. 164973.

[21] H. Xu, F. Li, Y. Gao, and W. Wang, "Simultaneous measurement of tilt and acceleration based on FBG sensor," *IEEE Sensors J.*, vol. 20, no. 24, pp. 14857–14864, Dec. 2020.

[22] D. Lapadatu, S. Habibi, B. Reppen, G. Salomonsen, and T. Kvisteroy, "Dual-axes capacitive inclinometer/low-g accelerometer for automotive applications," in *Proc. Tech. Dig. MEMS 14th IEEE Int. Conf. Micro Electro Mech. Syst.*, Jan 2001, pp. 34–37.

[23] C. H. Lee and S. S. Lee, "Study of capacitive tilt sensor with metallic ball," *ETRI J.*, vol. 36, no. 3, pp. 361–366, Jun. 2014.

[24] K. Rao *et al.*, "A high-resolution area-change-based capacitive MEMS tilt sensor," *Sens. Actuators A, Phys.*, vol. 313, Oct. 2020, Art. no. 112191.

[25] S. M. Khan, N. Qaiser, and M. M. Hussain, "An inclinometer using movable electrode in a parallel plate capacitive structure," *AIP Adv.*, vol. 9, no. 4, Apr. 2019, Art. no. 045118.

[26] R. Olaru and D. D. Dragoi, "Inductive tilt sensor with magnets and magnetic fluid," *Sens. Actuators A, Phys.*, vol. 120, no. 2, pp. 424–428, May 2005.

[27] S. Su, D. Li, N. Tan, and G. Li, "The study of a novel tilt sensor using magnetic fluid and its detection mechanism," *IEEE Sensors J.*, vol. 17, no. 15, pp. 4708–4715, Aug. 2017.

[28] J. K. Lee, J. C. Choi, and S. H. Kong, "All-polymer electrolytic tilt sensor with conductive Poly(dimethylsiloxane) electrodes," *Jpn. J. Appl. Phys.*, vol. 52, no. 6S, Jun. 2013, Art. no. 06GL01.

[29] R. S. Dahiya and M. Valle, *Robotic Tactile Sensing: Technologies and System*. Dordrecht, The Netherlands: Springer, 2013.

[30] D. Paczesny, G. Tarapata, M. Michał, and R. Jachowicz, "The capacitive sensor for liquid level measurement made with ink-jet printing technology," *Procedia Eng.*, vol. 120, pp. 731–735, Jan. 2015.

[31] A. Manut, A. S. Zoolfakar, N. A. Muhammad, and M. Zolkapli, "Characterization of inter digital capacitor for water level sensor," in *Proc. IEEE Regional Symp. Micro Nano Electron.*, Sep. 2011, pp. 359–363.

[32] E. Terzic, C. R. Nagarajah, and M. Alamgir, "Capacitive sensor-based fluid level measurement in a dynamic environment using neural network," *Eng. Appl. Artif. Intell.*, vol. 23, no. 4, pp. 614–619, Jun. 2010.

[33] B. Kumar, G. Rajita, and N. Mandal, "A review on capacitive-type sensor for measurement of height of liquid level," *Meas. Control*, vol. 47, no. 7, pp. 219–224, Sep. 2014.

[34] R. Geethamani, S. S. Rani Gnanamalar, N. Ramyarani, and C. Pavithra, "Non-contact continuous capacitive liquid level sensing," *Int. J. Pure Appl. Math.*, vol. 119, pp. 1921–1930, Apr. 2018.

[35] C. G. Núñez, L. Manjakkal, and R. Dahiya, "Energy autonomous electronic skin," *NPJ Flexible Electron.*, vol. 3, no. 1, pp. 1–24, Dec. 2019.

[36] Y. Guo, C. Li, X. Zhou, L. Jiang, and H. Liu, "Wide-range fiber Bragg grating tilt sensor based on a cam structure," *IEEE Sensors J.*, vol. 20, no. 9, pp. 4740–4748, May 2020.

[37] O. Ozioko, H. Nassar, C. Muir, and R. Dahiya, "3D printed capacitive tilt sensor," in *Proc. IEEE Int. Conf. Flexible Printable Sensors Syst. (FLEPS)*, Aug. 2020, pp. 1–4.

[38] W. Navaraj and R. Dahiya, "Fingerprint-enhanced capacitive-piezoelectric flexible sensing skin to discriminate static and dynamic tactile stimuli," *Adv. Intell. Syst.*, vol. 1, no. 7, Nov. 2019, Art. no. 1900051.

[39] H. Nassar, A. Pullanchiyodan, M. Bhattacharjee, and R. Dahiya, "3D printed interconnects on bendable substrates for 3D circuits," in *Proc. IEEE Int. Conf. Flexible Printable Sensors Syst. (FLEPS)*, Jul. 2019, pp. 1–3.

Oliver Ozioko received the B.Eng. degree in electronic engineering from the University of Nigeria, Nsukka, the master's degree in electronic/electrical engineering from the Federal University of Technology Owerri, Nigeria, in 2012, and the Ph.D. degree from the University of Glasgow, U.K. in 2019. He is currently a Postdoctoral Researcher with the Bendable Electronics and Sensing Technologies (BEST) Group, University of Glasgow. His current research interests include electronic skin, haptics, soft robotics, wearable tactile sensors and actuators for application in robotics, and assistive technologies.

Habib Nassar received the B.Eng. degree in electronic and communication engineering from the University of York, U.K., in 2016, and the M.Sc. degree in biomedical engineering from the University of Glasgow, U.K., in 2017, where he is currently pursuing the Ph.D. degree with the Bendable Electronics and Sensing Technologies (BEST) Group. His research interests include sensory prostheses, electronic sensors, 3D printing, and assistive robotics.

Ravinder Dahiya (Fellow, IEEE) is a Professor of Electronics and Nanoengineering with the University of Glasgow, U.K. He is also the Leader of the Bendable Electronics and Sensing Technologies (BEST) Research Group, which conducts fundamental and applied research in flexible electronics, tactile sensing, electronic skin, robotics, and wearable systems. He has authored over 350 research articles, seven books, and 15 submitted/granted patents. He has led several international projects. He is the President-Elect for the term of 2020 to 2021 and a Distinguished Lecturer of the IEEE Sensors Council. He is serving on the Editorial Board of the Scientific Reports. He was on the Editorial Board of IEEE SENSORS JOURNAL from 2012 to 2020 and IEEE TRANSACTIONS ON ROBOTICS from 2012 to 2017. He holds the prestigious EPSRC Fellowship and received in past the Marie Curie and Japanese Monbusho Fellowships. He has received several awards, including the 2016 Microelectronic Engineering Young Investigator Award (Elsevier), the 2016 Technical Achievement Award from the IEEE Sensors Council, and nine best paper awards as author/coauthor in conferences and journals. He was the Technical Program Co-Chair of IEEE SENSORS in 2017 and 2018 and a General Chair of several conferences, including IEEE FLEPS 2019, 2020, and 2021, which he founded.